4

Technical Document 1461
February 1989

Infrared Ship Signature Evaluation

H. G. Hughes

NAVAL OCEAN SYSTEMS CENTER
San Diego, California 92152-5000

E. G. SCHWEIZER, CAPT, USN
Commander

R. M. HILLYER
Technical Director

ADMINISTRATIVE INFORMATION

This work was performed by the Tropospheric Branch, Code 543, Naval Ocean Systems Center, for the Office of Naval Technology.

Released by
H. V. Hitney, Head
Tropospheric Branch

Under authority of
J. H. Richter, Head
Ocean and Atmospheric
Sciences Division

ACKNOWLEDGMENTS

Appreciation is extended to Douglas Jensen, who provided the airborne measurements of meteorological parameters, and to Merle R. Paulson, who assisted in the AGA measurements and computer programming. John Cook, Naval Environmental Prediction Research Facility, was responsible for providing the FORTRAN version of SHIPSIG. Also, I wish to thank Perry Ostrowski, Naval Surface Weapons Center, for many helpful discussions.

JG

REPORT DOCUMENTATION PAGE

1a. REPORT SECURITY CLASSIFICATION UNCLASSIFIED	1b. RESTRICTIVE MARKINGS
2a. SECURITY CLASSIFICATION AUTHORITY	3. DISTRIBUTION/AVAILABILITY OF REPORT Approved for public release; distribution is unlimited.
2b. DECLASSIFICATION/DOWNGRADING SCHEDULE	
4. PERFORMING ORGANIZATION REPORT NUMBER(S) Technical Document 1461	5. MONITORING ORGANIZATION REPORT NUMBER(S)
6a. NAME OF PERFORMING ORGANIZATION Naval Ocean Systems Center 6b. OFFICE SYMBOL (If applicable) Code 543	7a. NAME OF MONITORING ORGANIZATION
6c. ADDRESS (City, State and ZIP Code) San Diego, CA 92152-5000	7b. ADDRESS (City, State and ZIP Code)
8a. NAME OF FUNDING/SPONSORING ORGANIZATION Office of Naval Technology 8b. OFFICE SYMBOL (If applicable)	9. PROCUREMENT INSTRUMENT IDENTIFICATION NUMBER
8c. ADDRESS (City, State and ZIP Code) Arlington, VA 22217-5000	10. SOURCE OF FUNDING NUMBERS PROGRAM ELEMENT NO. 62435N PROJECT NO. RM35G80 TASK NO. NO2C/2 AGENCY ACCESSION NO. DN488 760

11. TITLE (include Security Classification)

INFRARED SHIP SIGNATURE EVALUATION

12. PERSONAL AUTHOR(S)

H. G. Hughes

13a. TYPE OF REPORT	13b. TIME COVERED	14. DATE OF REPORT (Year, Month, Day)	15. PAGE COUNT
Interim	FROM TO	February 1989	22

16. SUPPLEMENTARY NOTATION

17. COSATI CODES			18. SUBJECT TERMS (Continue on reverse if necessary and identify by block number)
FIELD	GROUP	SUB-GROUP	Forward Looking Infrared (FLIR) Advanced Very High Resolution Radiometer (AVHRR)

19. ABSTRACT (Continue on reverse if necessary and identify by block number)

A case study is presented to test the ability of the computer code SHIPSIG (developed by the Naval Surface Warfare Center) to predict the zero-range average temperature for a Frigate-class ship during different meteorological conditions. The course of a guided missile frigate operating off the coast of San Diego, California, was chosen for this investigation. During a 5-hour period, changes in the ship's heading allowed solar heating of different sides of the ship. Using meteorological parameters measured on shore, the calculated ship's temperature response was found to respond favorably to the changes in solar heating. As the ship returned to harbor, its average temperature was measured as it passed close to a calibrated thermal imaging system. The predicted and measured (adjusted for atmospheric effects) average temperatures agreed within less than 2°C depending upon the surface emissivity of the ship. The sensitivities of the modeled temperatures to uncertainties in the meteorological input parameters are also discussed.

20. DISTRIBUTION/AVAILABILITY OF ABSTRACT ☐ UNCLASSIFIED/UNLIMITED ☒ SAME AS RPT ☐ DTIC USERS	21. ABSTRACT SECURITY CLASSIFICATION UNCLASSIFIED
22a. NAME OF RESPONSIBLE PERSON H. G. Hughes	22b. TELEPHONE (include Area Code) (619) 553-1418 22c. OFFICE SYMBOL Code 543

CONTENTS

FIGURES

INTRODUCTION

The standoff ranges at which an adversary can detect and/or track a surface ship using infrared sensors are of primary importance for a ship commander to estimate the time allowable for evasive actions against guided weaponry launched at the ship or for the deployment of countermeasures. Algorithms presently operational in the U. S. Navy (CSC, 1986, and STX Corp., 1988) for predicting the performance of an airborne Forward Looking Infrared (FLIR) system operating against a surface target require as an input the radiometric temperature difference between the target and its natural background. The algorithms determine the range at which the temperature difference is degraded by the atmospheric infrared transmittance to the minimum detectable temperature difference of the sensor system. The effective blackbody temperature of the sea background can be determined using the atmospheric transmittance and radiance computer code LOWTRAN 6 (Kneizys et al., 1983) which has been modified by Wollenweber (1988) to account for the contributions to the background by sky reflections and emissions from a wind-ruffled sea surface. Computer codes are presently available such as SIREOS (Burns, et al., 1980) (three-dimensional) and SIRS (Batley, 1978) (two-dimensional), which are capable of using several hundred individual structural elements of a ship to model its composite infrared signature. However, these codes are quite complex and require extensive running times, making them impractical for shipboard use in a real-time prediction system.

A modification to the SIRS computer code has recently been developed at the Naval Surface Weapons Center. This modification, SHIPSIG (Ostrowski and Wilson, 1985), approximates the complex structure of a ship with plane elements which represent the ship's temperature at zero range on an average basis. For a given viewing direction, the simplest representation of a ship consists of a single vertical and horizontal element with the observer's orientation accounted for by appropriate area components. The infrared signature calculations are then based on a thermodynamic analysis of both elements individually. They are combined by scaling the element radiance in proportion to the ship area each represents. In the present model, the horizontal and vertical elements and ship stack correction factors applied to the vertical element are for a guided missile, frigate-class ship. The original BASIC version of the code has been rewritten in FORTRAN language for the HP-9020 computer. The model requires as inputs the ship's course and speed as a function of time from a starting geographic latitude, the surface wind speed and direction, visibility, relative humidity, air temperature, the ship's initial temperature, and the viewing angle. Comparisons (Ostrowski and Wilson, 1985) of the SHIPSIG calculations with the more detailed SIRS code have shown good agreement in average ship temperatures for modeled ship courses and weather conditions. However, the single-element model has not yet been validated using an actual target, nor has the sensitivity of the ship temperature predictions to the meteorological input parameters been addressed.

In this report, a case study is presented to test the model's ability to predict the average temperature of a guided missile frigate after a 5-hour cruise at sea during which course changes allowed solar heating of different sides of the ship. For these measurements, a calibrated thermal imaging system (AGA Model 780 THERMO

VISION) was used to make closeup measurements of the ship as it passed near the sensor when the ship returned to harbor. In the following sections, the measurement of the average ship temperature is discussed and compared with the model predictions. A sensitivity analysis is also presented of the calculated average ship temperature as a function of time to the meteorological input parameters. The method by which the atmospheric effects are removed from the AGA measurements is discussed in the appendix.

MEASUREMENTS AND CALCULATIONS OF AVERAGE SHIP TEMPERATURE

Figure 1 shows the course of a guided missile frigate, the USS *Brooke* (FFG 1), chosen to demonstrate the model, off the coast of San Diego, California, on 9 June 1988. During the 5-hour period, changes in the ship's heading allowed solar heating of different sides of the ship. As the ship completed the course and returned to harbor, it passed close to the AGA thermal imaging system located at an altitude of 30 m on shore about 2 km from channel buoy #6 near the entrance to the harbor. The AGA measurements (8 to 12 μm) were made using a 2.95° field-of-view lens with an instantaneous field of view of 0.87 mr. The response of the system was determined by placing a blackbody of known temperature (± 0.1°C for temperatures <50°C) in front of the lens aperture. The digitized video signal transfer function of the system then allowed the blackbody temperature to be reproduced to within ± 0.2°C. Figure 2 is the thermogram taken with the AGA system as the ship entered the harbor. The AGA system's data processing software allows subtraction of the sea background radiance surrounding the ships and provides a histogram of the temperature distribution of the ship pixels within the chosen rectangular areas, as shown in the inset to the right of each ship. Temperatures on the histogram (percentage of total number of pixels in a temperature band) are shown in the color corresponding to the bar on the temperature scale to the left. The mean temperature (uncorrected for atmospheric effects) was 19.7°C. Superimposed on the histogram is a Gaussian curve (represented by dots) which best fits the temperature points. The temperature distribution approximates the Gaussian points remarkably well.

The measured radiance, N(meas), of the ship at a range R is related to its actual effective blackbody radiance, N(ship), and the atmospheric emission, N(path), along the path by

$$N(\text{meas}) = N(\text{ship})\tau(R) + N(\text{path}) \tag{1}$$

where $\tau(R)$ is the atmospheric transmittance at a range R. The range to the ship was determined to be approximately 1.7 km using the known vertical dimensions of the ship and their angular subtense within the field of view of the AGA. LOWTRAN 6 calculations of transmittance and path emission were made to determine the temperature equivalent to N(ship). In the calculations, the Navy Maritime Aerosol Model was chosen to include the effects of aerosols. This model requires the inputs of surface wind speeds (current and 24-h averaged), relative humidity, surface visibility, and an air mass factor which identifies the origin of the aerosols as either marine or continental and is allowed to range between integer values of 1 for open ocean to 10 for coastal regions. The method by which the representative aerosol parameters for this data set were chosen is discussed in appendix A. Basically, the measured surface wind speeds and airborne measurements of temperature, pressure, and relative humidity are used in LOWTRAN calculations to determine the appropriate combinations of visibility and air mass factors which allow agreement with the horizon pixel radiance as measured by the AGA system. In the LOWTRAN

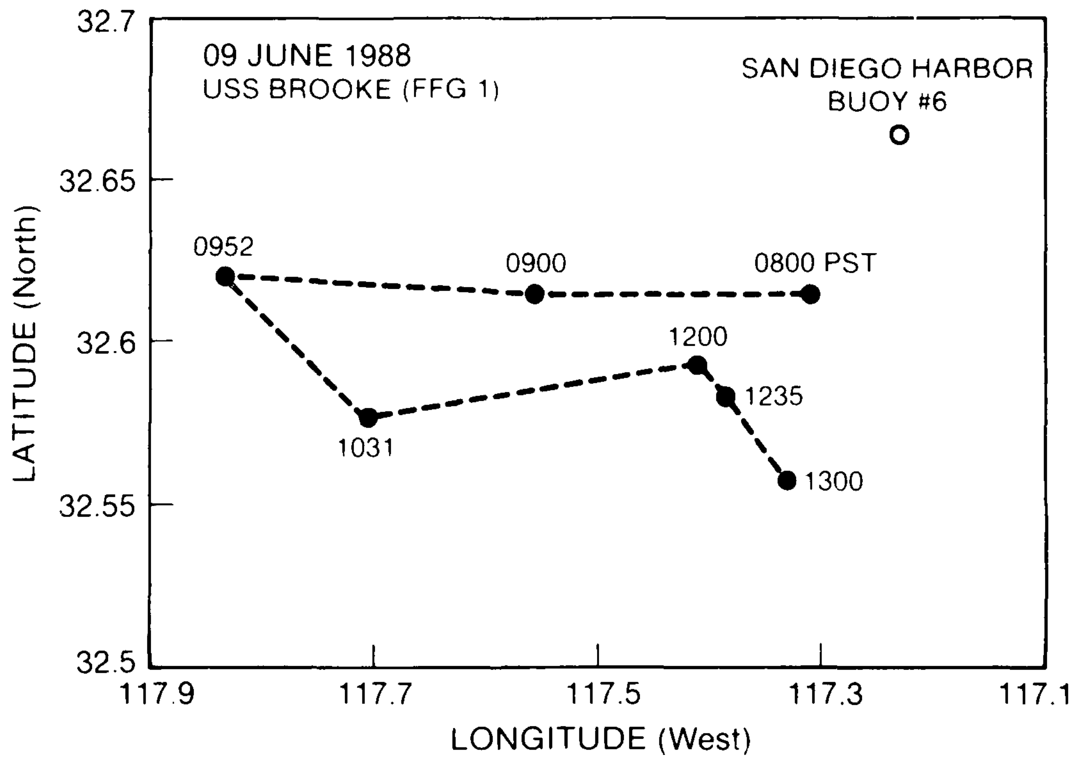

Figure 1. Course of the USS *Brooke* (FFG 1) on 9 June 1988.

calculations, the relative humidity (72 percent), air temperature (20°C), pressure (1012.4 mb), current wind speed (2.9 m/s), 24-h averaged wind speed (2.8 m/s) measured on the Point Loma Peninsula were used with the air mass factor (integer value of 3) and visibility (37 km) as selected from the horizon comparisons. These calculations resulted in an adjusted AGA average temperature measurement of 20.5°C, assuming the surface emissivity (ϵ) of the ship was unity.

For the model calculations, the initial position of the ship was taken to be near the entrance to San Diego harbor. The initial ship temperature, its ambient temperature, and relative humidity throughout the course were not recorded by the ship. These values were taken to be constants as measured at the AGA site. The surface wind was southwesterly (252°True), and the depression angle of viewing was essentially broadside at 0.6°. The average ship temperatures calculated for the port and starboard sides of the ship as a function of time are shown in figure 3. The most

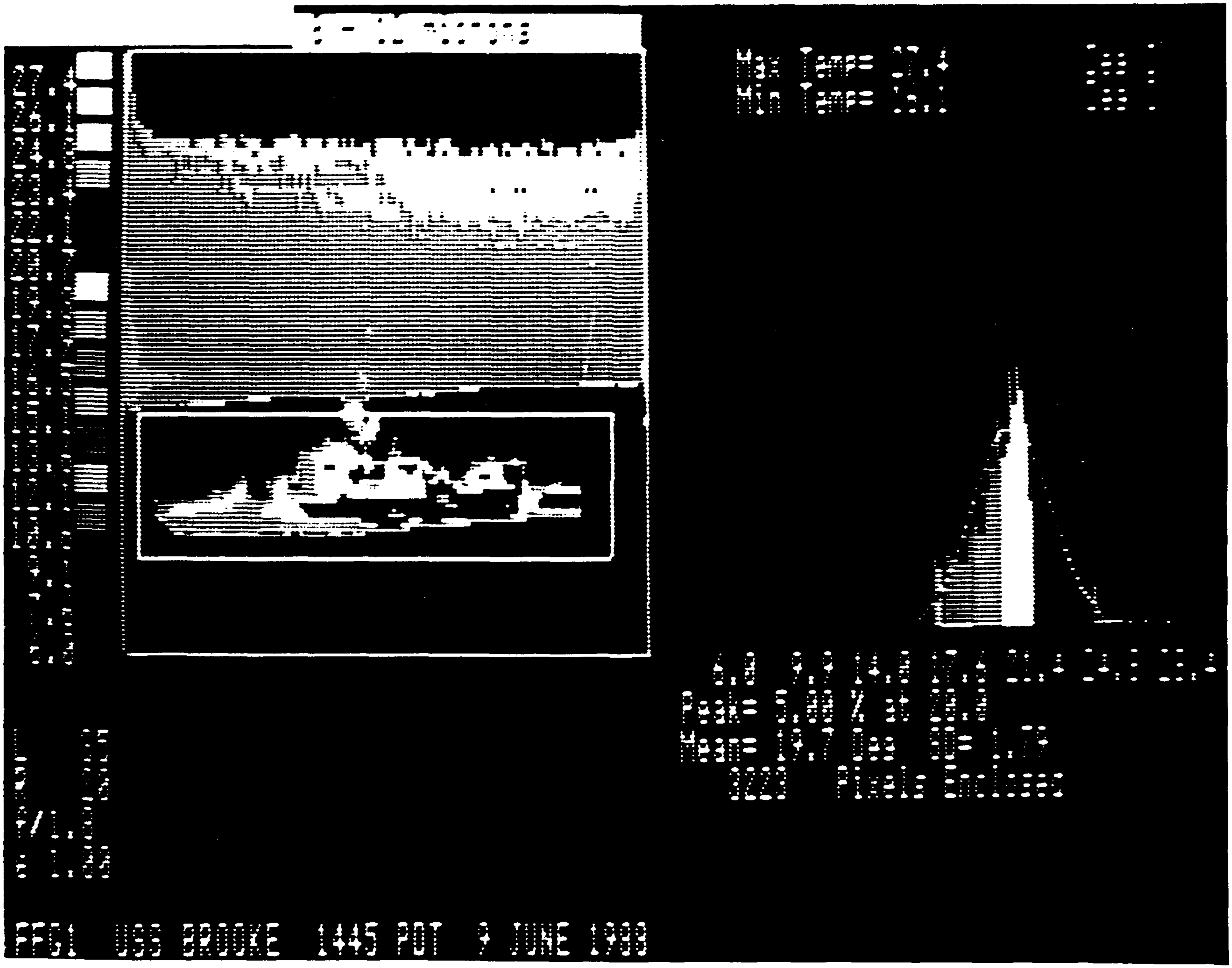

Figure 2. Infrared thermogram of the USS Brooke (FFG 1) as it entered San Diego Harbor on 9 June 1988.

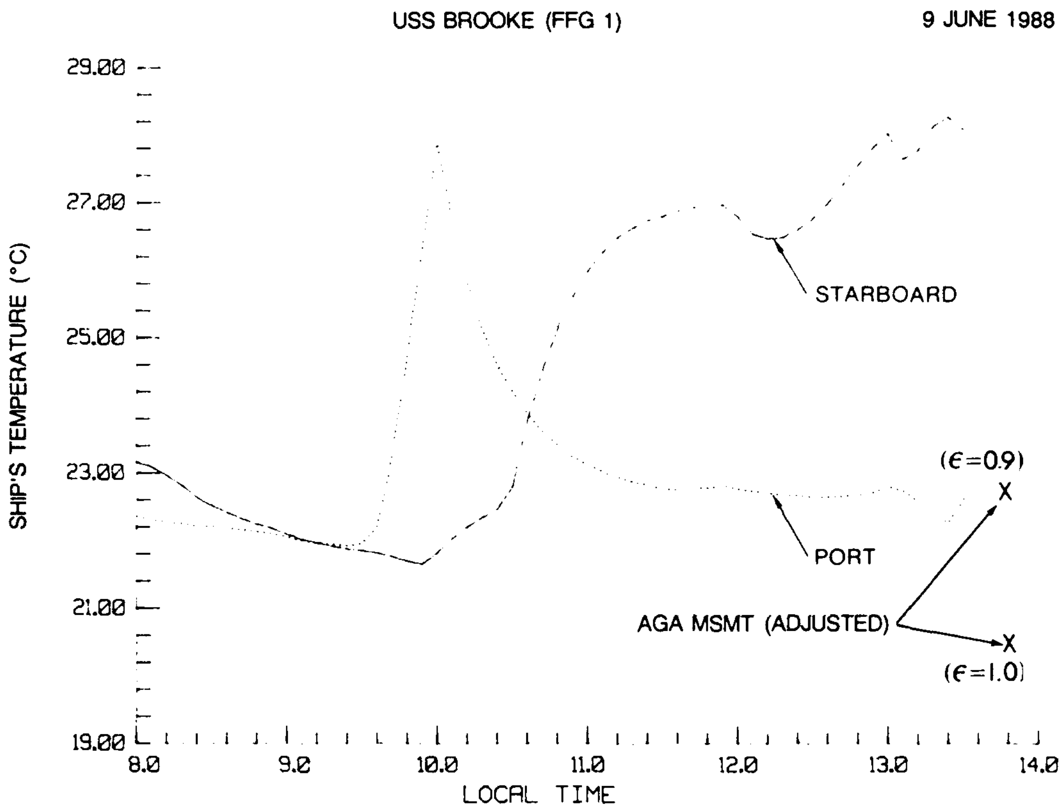

Figure 3. Comparison of the average temperature of the port side of the USS *Brooke* (FFG 1) with the adjusted AGA measurements as the ship entered San Diego harbor.

apparent features in the temperature responses are the gradual heating of the port side and cooling of the starboard side as the ship steamed westward in the early morning, and their abrupt cooling and heating after 1000 hours following the southeasterly course change at 0952 hours. The magnitude of the port side average temperature is approximately 2°C greater (for an emissivity of unity) than that measured by the AGA system as it returned to harbor near 1345 hours. If indeed the emissivity of the ship was 0.9, as is assumed in the model, the measured average temperature would be in better agreement (22.7°C).

SENSITIVITY TO METEOROLOGICAL PARAMETERS

The solar heating of each element is calculated according to its orientation and time of day. The atmospheric transmission of solar energy is governed by the humidity and visibility input parameters. Convective cooling coefficients resulting from the prescribed motion of the ship are also calculated on the basis of empirical relationships between the ship and wind velocities and the ambient air temperature. While conductive cooling/heating by the seawater most certainly would affect the ship's temperature, it is not included in the calculations. It is not possible here to determine the myriad of combinations of the input parameters' uncertainties which will affect the calculated ship temperature. In this section, we will examine the response of the model (port side temperatures) to uncertainties in a single meteorological parameter under cloud free skies during daytime, while the remaining parameters are held constant at the values used in the calculations of figure 3.

Figure 4 shows the response of the calculated ship temperature's differing ambient air temperatures of 18°C, 19°C, and 20°C. While the shapes of the response curves do not appear to be sensitive, their magnitudes differ by amounts equivalent to the uncertainties.

Figure 5 shows the sensitivity to the visibility input. The temperature response of the ship before 1100 hours is quite different for a 5-km visibility as compared to 25 and 40 km, and the magnitude of the response at the time of the first course change is approximately 4°C less. The reason for the slightly higher temperature at 25 km visibility over that at 40 km is not understood.

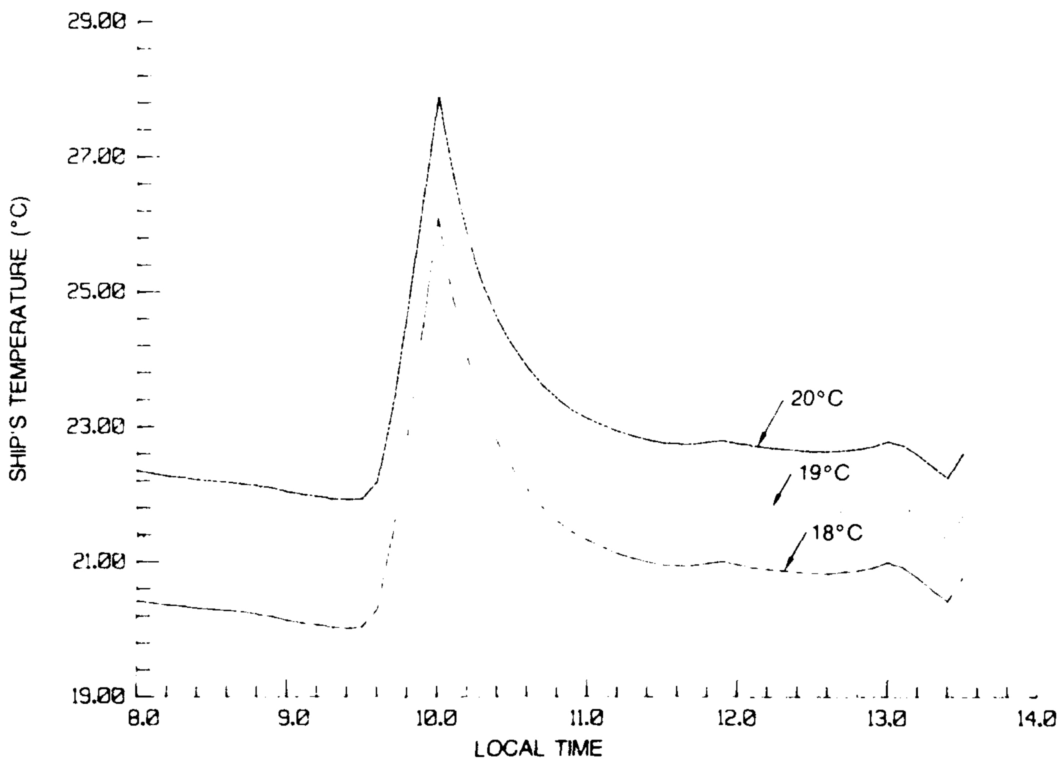

Figure 4. Calculated ship's temperature versus local time for different ambient air temperatures.

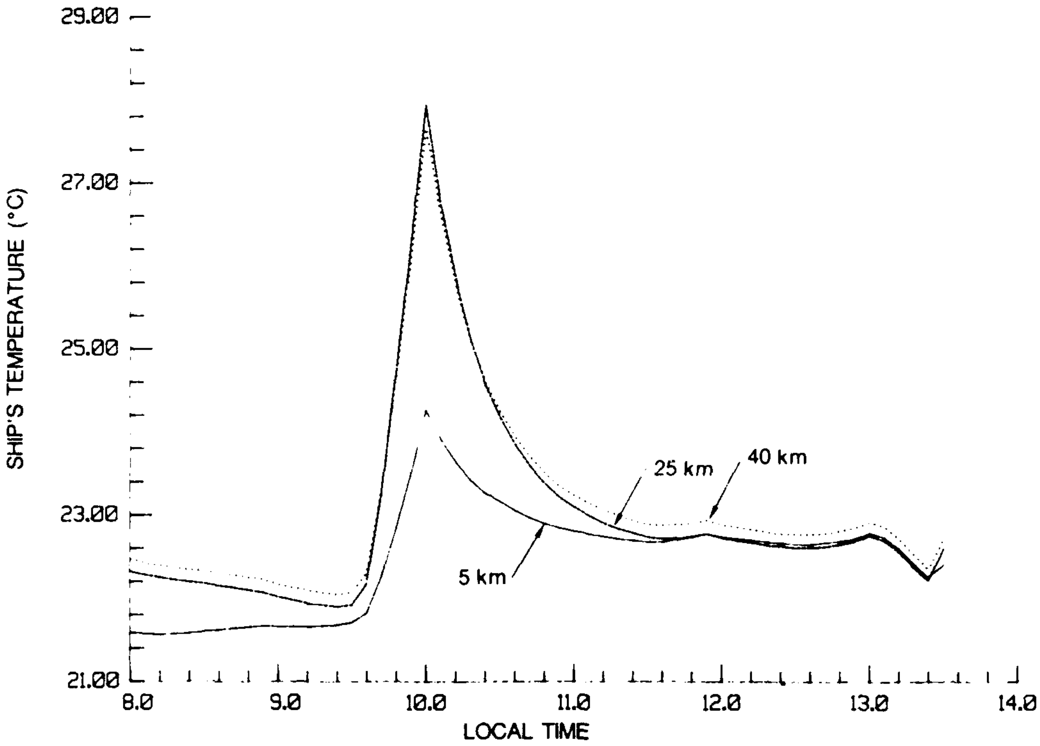

Figure 5. Calculated ship's temperature versus local time for different surface visibilities.

The insensitivity of the response to differing values of relative humidity (50, 70, and 90 percent), shown in figure 6, is related to the solar insolation properties of the atmosphere, which are primarily determined by the absorption and scattering properties of aerosols rather than water vapor absorptions at the shorter wavelengths.

Figures 7 and 8 show the responses to surface winds of 2, 7, and 14 m/s for directions differing by 90° (252°T as measured on shore and 342°T). While variation in wind speeds result in 1°C to 2°C differences in temperature, there is little difference between the responses for the two directions.

The look angle (depression below horizontal) is apt to be the most accurately defined input parameter. However, the temperature response is quite sensitive to changes in this parameter. The responses to look angles of 0°, 2°, and 5° are shown in figure 9. In this example, the increase in ship's temperature after 1000 hours with increasing look angle is a result of the increased aspect area contributed by the horizontal element, which was more exposed to the sun than the vertical element.

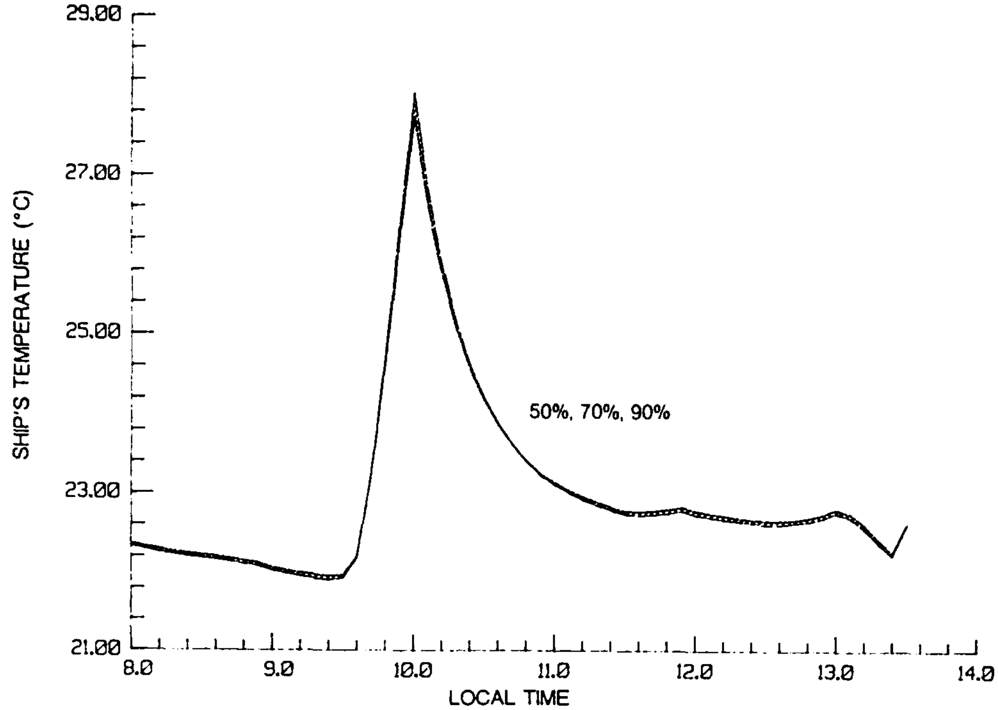

Figure 6. Calculated ship's temperature versus local time for different relative humidities.

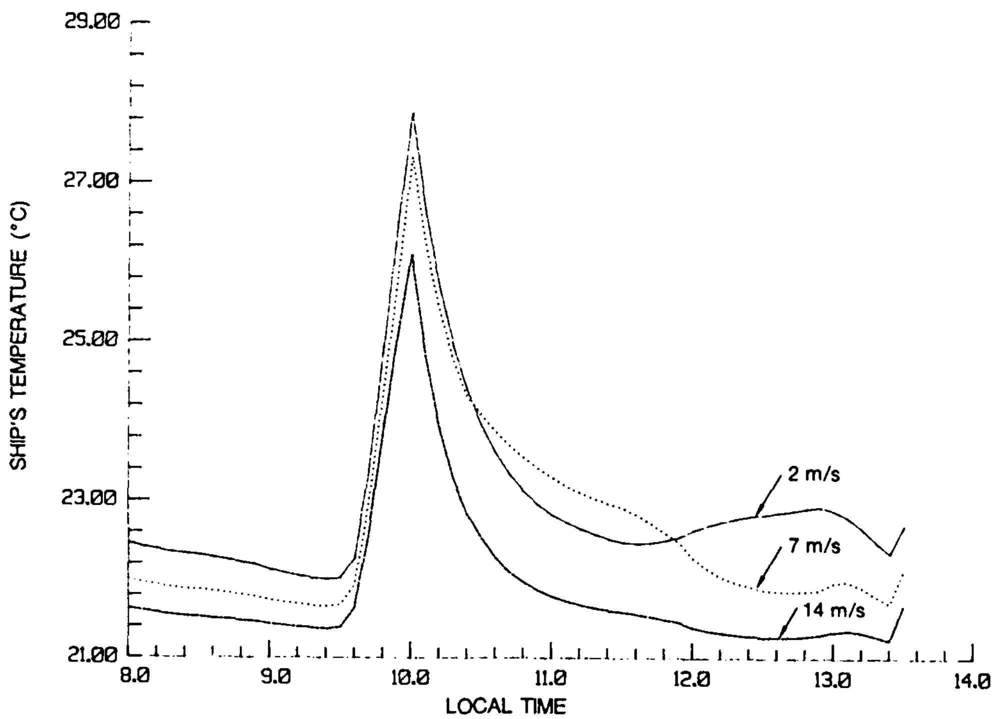

Figure 7. Calculated ship's temperature versus local time for different surface wind speed and wind direction of 252°T.

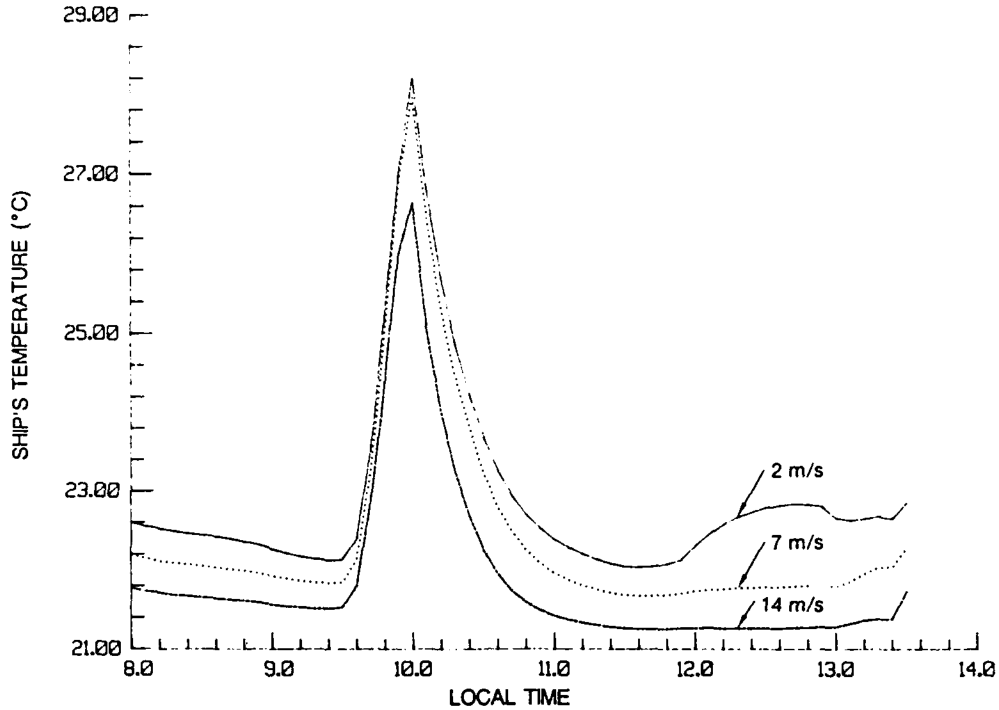

Figure 8. Calculated ship's temperature versus local time for different surface wind speeds and wind direction of 342°T.

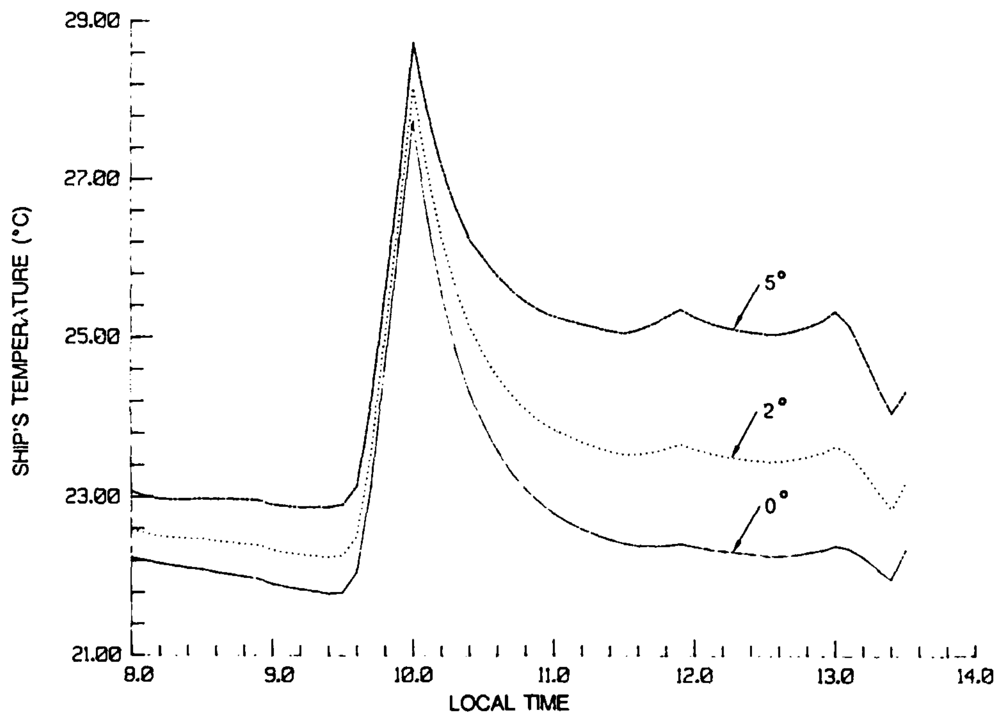

Figure 9. Calculated ship's temperature versus local time for different look angles.

DISCUSSION AND RECOMMENDATIONS

This preliminary evaluation of the ship temperature model shows promise that it responds well to the differing solar heating conditions. Allowing for the uncertainties in the meteorological parameters surrounding the ship throughout its course and the approximations inherent in the model itself, the relatively small difference between the modeled and measured average temperatures of the ship as it entered harbor is gratifying.

The most critical input parameters to the model have been shown to be the ambient (as well as the initial) air temperature of the ship and surface visibility. The ship's course and speed and the wind are also critical factors and need to be accurately accounted for on board the ship. Further measurements need to be performed with "ground-truth" measurements of the radiometric temperature of selected portions of the ship to test the accuracy by which the AGA measurements can be adjusted to retrieve the actual ship's temperature. A further test of the model should include operational FLIR systems to test its use in performance prediction codes.

REFERENCES

Batley, P. E. (1978). *Ship Infrared Signatures (SIRS) Computer Model – Technical Overview and User's Manual.* David Taylor Naval Ship Research and Development Center Report SME-78-37.

Burns, R. H. et al. (1980). *Description of the Ship Infrared/Electro-Optical Scenario (SIREOS) Computer Model.* David Taylor Naval Ship Research and Development Center Report 80/097.

Computer Sciences Corporation (1986). *Forward Looking Infrared Performance Function Program Performance Specification (PPS) for the Tactical Environmental Support System (TESS).* NOSC TD 1000.

Hughes, H. G. (1987). "Evaluation of the LOWTRAN 6 Navy Maritime Aerosol Model Using 8 to 12 μm Sky Radiances," *Opt. Eng.*, 26, 1155.

Kneizys, F. X., E. P. Shettle, W. O. Gallery, J. H. Chetwynd, Jr., J. H. Abreu, J. E. A. Selby, S. A. Clough, and R. W. Fenn (1983). *Atmospheric Transmittance/Radiance: Computer Code LOWTRAN 6.* Air Force Geophysics Laboratory Technical Report No. 83-0187.

Ostrowski, P. P., and D. M. Wilson (1985). *A Simplified Computer Code for Predicting Ship Infrared Signatures.* NSWC TR 84-540.

STX Corporation (1988). *FLIR Program Upgrade – Users Manual,* NEPRF Document 5W0513, UM-40.

Wollenweber, F. G. (1988). *Infrared Sea Radiance Modeling Using LOWTRAN 6.* NOSC TD 1355.

APPENDIX A
SELECTION OF ATMOSPHERIC AEROSOL MODEL FOR AGA TEMPERATURE ADJUSTMENTS

For this study, a Piper Navajo aircraft, equipped with Rosemount temperature and pressure probes and an EG&G dewpoint sensor, made a vertical spiral over the ocean to obtain the profile of temperature, relative humidity, and pressure which are required inputs to the LOWTRAN 6 computer code. The vertical profiles of temperature and relative humidity, which were measured at 1330 PST on 9 June 1988, approximately 9 km off the coast of San Diego, California, are shown in figure A-1. The profiles extending up to an altitude of 2700 m were divided into 33 layers as allowed by LOWTRAN 6. The lower layers of the profiles are also divided into sublayers containing the same amount of absorbing and scattering material and the temperature as the original layer. This artificial layering has been found necessary to remove the anomalous dip which occurs when aerosols are included in the LOWTRAN 6 radiance calculations for zenith angles close to 90°.

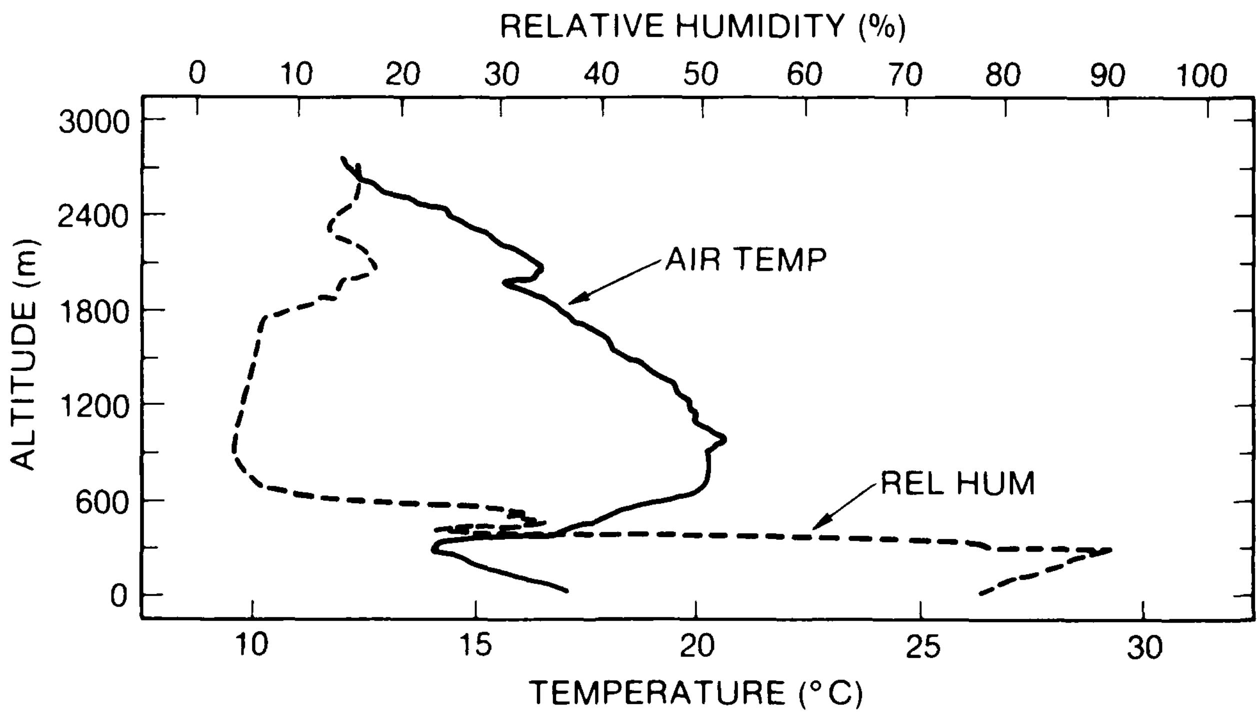

Figure A-1. Profiles of air temperature and relative humidity measured with altitude on 9 June 1988 off the coast of San Diego.

The LOWTRAN 6 aerosol model chosen for the calculations is the Navy Maritime Aerosol Model. This model is the sum of three lognormal size distributions and, in addition to the surface wind speeds (current and 24-h averaged) and relative humidity, requires the input of an air mass factor which identifies the origin of the aerosols as either marine or continental and is allowed to range between integer values of 1 for open ocean to 10 for coastal regions. Also, when an observed surface visibility is available as an input, the model is adjusted so that the calculated visibility at a wavelength of 0.55 μm is the same as the observed value. The air mass factor is defined in terms of atmospheric radon content or an air mass trajectory analysis to determine the time the air mass has been over land. As neither of these techniques was available, an alternate method was used to select an appropriate air mass factor. Near the time the meteorological parameters were obtained, measurements of IR (8 to 12 μm) horizon radiances were made with the calibrated AGA thermal imaging system. For these measurements, the scanner was located at an elevation of 30 m on the Point Loma peninsula and was directed in a southerly direction over the ocean such that approximately half of the field of view was above and half below the horizon. The measured radiance scene is shown in figure A-2. The data processing software of the AGA system allows the effective blackbody temperature of each pixel in the scene to be displayed on the computer terminal screen, and, in this case, the horizontal cursor is situated on the pixel corresponding to the maximum temperature (16.5°C or 3.23 mW/cm^2 sr) in the scene which is taken to coincide with the infrared horizon. The temperatures of the different colors in the scene are also identified by the color bars displayed on the left which correspond to the midpoints of the temperatures printed above and below each bar. Using the current and 24-h averaged wind speeds (V_C = 2.9 m/s and $\bar{V}$= 2.8 m/s) measured on shore and the vertical profiles of meteorological parameters measured by the aircraft, LOWTRAN 6 calculations were made to agree with the maximum pixel radiance in the scene using nonunique combinations of air mass factors and visibilities. (Note that these calculations were made using a modified current wind speed component, $A_3 = 10^{(0.06V_c - 2.8)}$, which is different from the value published in LOWTRAN 6. This modification was found to be necessary to match previously published measurements of IR sky radiances and near-surface aerosol size distributions (Hughes, 1987) using the model). As the AGA scanner could not be accurately plumbed, the zenith angle of the infrared horizon was taken be 0.01° less than the angle for which the LOWTRAN calculations indicated the refracted ray path first hit the earth. In this case, the zenith angle corresponding to maximum radiance is 90.17°.

In figure A-3, the solid line represents the locus of points which allows the LOWTRAN calculations to match the measured horizon pixel radiance with the different combinations of air mass factors and visibilities. At the time of the measurements, Los Coronados coastal islands off San Diego were barely visible to the naked eye at ranges between 25 and 35 km. In the figure, the integer values of 3 and 4 correspond to visibilities close to these ranges of 23 and 37 km respectively. The range to the ship was determined to be approximately 1.7 km using the known vertical dimensions of the ship and their angular subtense within the field of view of the AGA. The relative humidity (72 percent), air temperature (20°C), and pressure (1012.4 mb) measured at the AGA location were used in LOWTRAN 6 calculations of transmittance and path emission to determine the temperature equivalent to N(ship). Figure A-4 shows the adjusted temperature dependence on visibility and air mass (AM) factor. Conveniently, both of the combinations of air mass factor and visibility (AM = 3, visibility = 37 km, and AM = 4, visibility = 23 km) result in the same adjusted ship's temperature of 20.5°C for a surface emissivity of unity. Had the ship's emissivity been 0.9, as is assumed in SHIPSIG, the adjusted temperature would be 22.7°C.

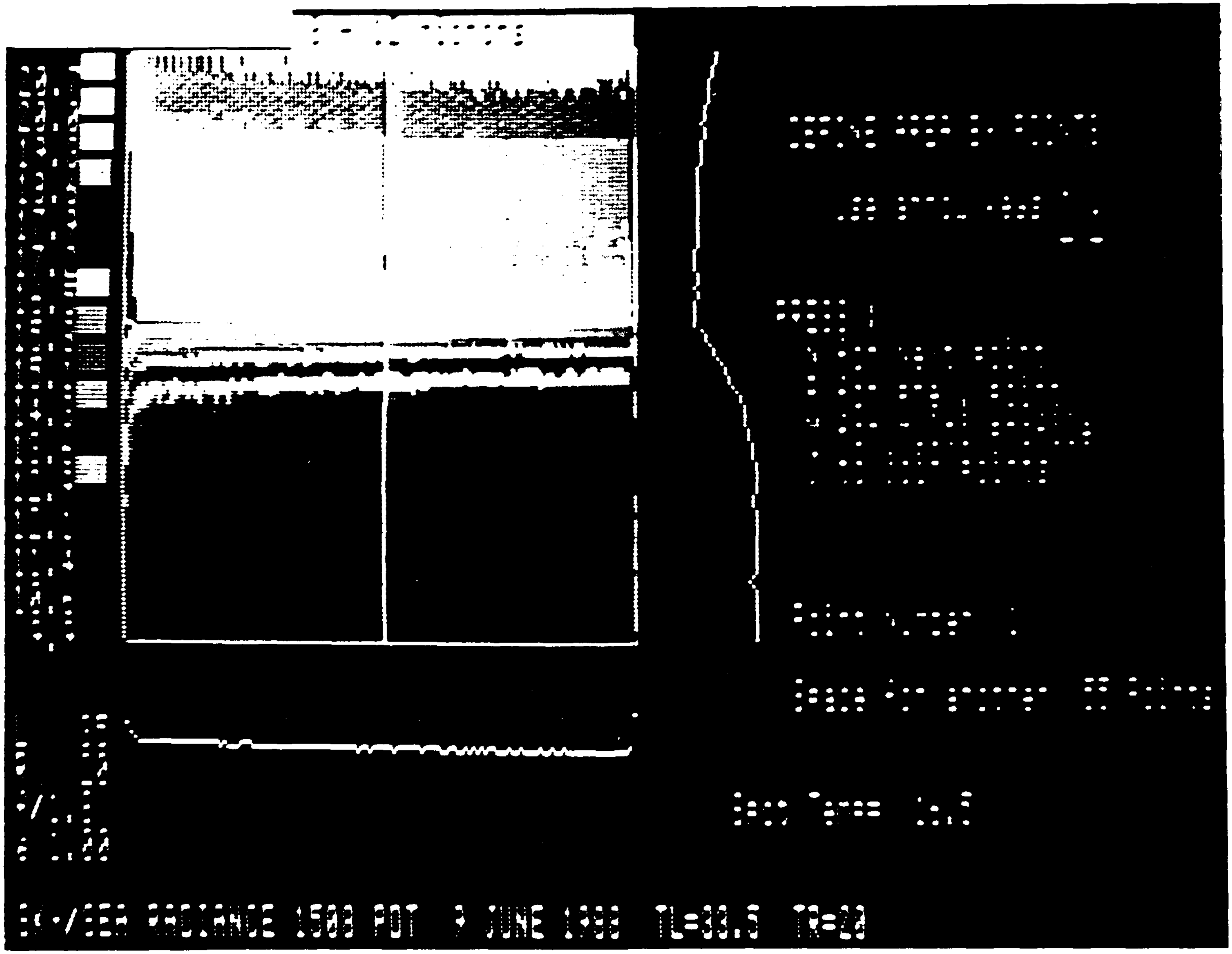

Figure A-2. Thermogram of near horizon infrared (8 to 12 μm) radiances measured over the ocean on 9 June 1988.

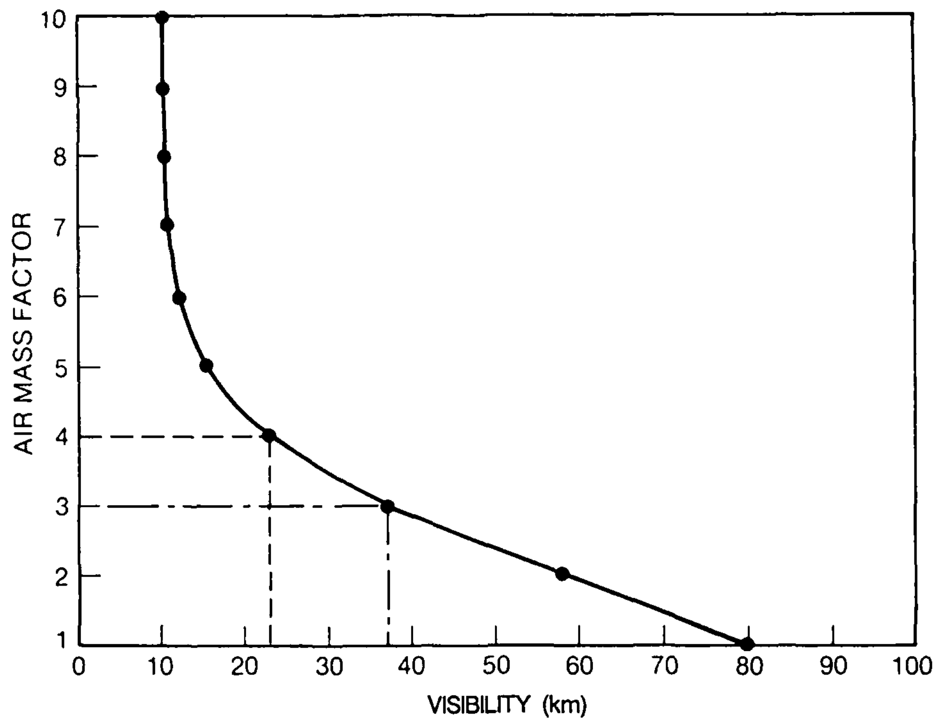

Figure A-3. Locus of points of LOWTRAN 6 calculations with different combinations of air mass factors and visibilities which match the measured infrared horizon radiance in figure A-2.

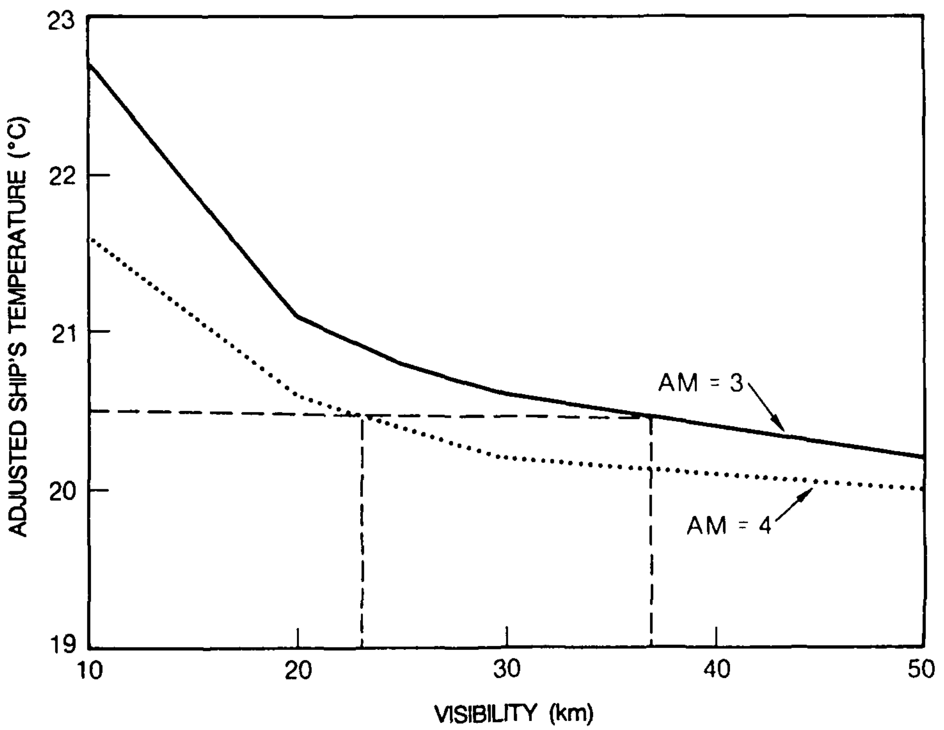

Figure A-4. Ship's average temperature adjusted for atmospheric effects versus visibility for different AM factors.